Supplement of Atmos. Chem. Phys., 21, 6875–6893, 2021
https://doi.org/10.5194/acp-21-6875-2021-supplement

Supplement of

Present-day radiative effect from radiation-absorbing aerosols in snow

Paolo Tuccella et al.

Correspondence to: Paolo Tuccella (paolo.tuccella@aquila.infn.it, paolo.tuccella@univaq.it)

1. GEOS-Chem setup and RAA treatment

BC and primary organic aerosols (POA) were calculated according to Park et al. (2003). SOAs were parameterized by using the scheme of Pye et al. (2010), while dry deposition was simulated with a resistance-in-series model (Zhang et al., 2001). Finally, the wet deposition processes were parameterized through the scheme from Liu et al. (2001) and included the both the below-cloud washout from large-scale and convective precipitation, and in cloud removal for stratiform clouds and convective updrafts.

Primary anthropogenic emissions of BC and POA were taken from Bond et al. (2007) inventory. Global anthropogenic emissions of CO, NO_x, and SO_x were taken from Emissions Database for Global Atmospheric Research (EDGAR) v4.2 (1° × 1°) (Olivier & Berdowski, 2001). The volatile organic carbon (VOC) emissions were from the REanalysis of the TROposhperic chemical composition (RETRO) (0.5° × 0.5°) inventory (Schultz et al., 2007). Regional inventories were used to replace EDGAR and RETRO, such as: EMEP (50 km × 50 km) (Vestreng et al., 2007) for Europe, NEI2011 (12 km × 12 km) ((http://www.epa.gov/ttnchie1/net/2005inventory.html) for the United States, BRAVO (0.1° × 0.1°) (Kuhns et al., 2005) for Mexico, CAC (0.1° × 0.1°) (http://www.ec.gc.ca/inrp-npri/) for Canada, and Streets et al. (2003) data (1 km × 1 km) for Asia.

The biomass burning emissions of BC and POA followed the year-specific daily mean GFED4s (Global Fire Emissions Database with small fires) inventory (van der Werf et al., 2010; Giglio et al., 2013), while the biogenic emissions were calculated interactively within GEOS-Chem, with the Model of Emissions of Gases and Aerosols from Nature (MEGAN) (Guenther et al., 2006). Dust emission flux was simulated through the Dust Entrainment And Deposition (DEAD) scheme (Zender et al., 2003), and the dust source function taken from the Goddard Chemistry Aerosol Radiation and Transport (GOCART) model (Ginoux et al., 2001; Chin et al., 2004).

We used a modified version of GEOS-Chem which included a specific treatment for RAAs, following our previous work (Tuccella et al., 2020). BC emissions and ageing were considered as source-dependent as in Wang et al. (2014, 2018) and hydrophobic and hydrophilic BC were tracked for FF, BF, and BB sources. According to Wang et al. (2014), 80% of BC from FF sources was emitted as hydrophobic and converted to hydrophilic with an ageing rate depending on sulphate dioxide and hydroxyl radical levels in the atmosphere (Liu et al., 2011). By contrast, BC from BF and BB sources was assumed to be emitted as 70% hydrophilic and 30% as hydrophobic with an ageing e-folding time from hydrophobic to hydrophilic of 4 hours.

As in Wang et al. (2014), BrC emissions were inferred from POA emissions, assuming 50% and 25% of POA from BF and BB emission as primary BrC. Moreover, we have assumed that half of emitted BrC is hydrophobic, with a conversion time of hydrophobic BrC to hydrophilic of 1.15 days.

BrC SOA is produced by many sources. Some studies showed as absorbing SOA is contained in aromatic compounds (Lambe et al., 2013), however, it may also derive from browning of some anthropogenic and biogenic SOA by reaction with ammonium, from photooxidation of α-pinene and toluene in the presence of NO_x and from the reaction of limonene with O_3 (Bones et al., 2010; Updyke et al., 2012). Other sources of BrC are aliphatic compounds (Laskin et al., 2015; Guang-Ming et al., 2016) and aqueous-phase chemical reactions in clouds (Zhang et al., 2017). The fraction of absorbing SOA in atmosphere is not well constrained, thus we assumed that all SOAs simulated by GEOS-Chem are BrC, following Lin et al. (2014). These, include: compounds from photooxidation of light aromatics, aerosol formed from photooxidation, ozonolysis, nitrate radical oxidation of monoterpenes and sesquiterpenes and products of isoprene oxidation (Pye et al., 2010).

Dust mass was simulated with four dimensional bins, with the following diameter boundaries: 0.2–2.0, 2.0–3.6, 3.6–6.0 and 6.0–12.0 µm. Emitted dust was distributed among these bins following Kok (2011). Dust emission was adjusted to give a global mean burden of 20 Tg which is the central estimate reported by Kok et al. (2017), calculated from observational constraints. Further details are provided in Tuccella et al. (2020).

2. BrC mass absorption efficiency

MAC_{BrC} has been inferred starting from the MAC of BF and BB absorbing OA reported by Wang et al. (2018). MAC_{OA} at 440 nm used for the BF was 0.76 m^2/g. For freshly emitted (hydrophobic) BB, MAC_{OA} at 440 nm was 0.77 m^2/g. According to Wang et al. (2018), we applied a reduced MAC_{OA} for aged (hydrophilic) OA of 0.23 m^2/g. We have used two different MAC_{OA} for freshly emitted and aged BB OA in order to take into account the whitening of BB plumes (Forrister et al., 2015).

Following again Wang et al. (2018), MAC_{OA} was translated to MAC_{BrC} using the relationship:

$$MAC_{OA} * Mass_{OA} = MAC_{BrC} * f * MAC_{OA}$$

where f is the assumed BrC fraction of OA mass. In our work, BrC was set to 50% and 25% for BF and BB OA, respectively. The resulting MAC_{BrC} values at 440 nm were 1.56, 3.08, and 0.92 m^2/g for BF, fresh and aged BB, respectively.

References

Bond, T. C., Bhardwaj, E., Dong, R., Jogani, R., Jung, S. K., Roden, C., Streets, D. G., Trautmann, D. G.: Historical emissions of black and organic carbon aerosol from energy-related combustion, Global Biogeochem., 21, 1850–2000, https://doi.org/10.1029/2006GB002840, 2007.

Bones, D. L., Henricksen, D. K., Mang, S. A., Gonsior, M., Bateman, A. P., Nguyen, T. B., Cooper, W. J., Nizkorodov, S. A.: Appearance of strong absorbers and fluorophores in limonene-O3 secondary organic aerosol due to NH4+ mediated chemical aging over long time scales, J. Geophys. Res., 115, https://doi.org/10.1029/2009JD012864, 2010.

Chin, M., Chu, A., Levy, R., Remer, L., Kaufman, Y., Holben, B., Eck, T., Ginoux, P., Gao, O.: Aerosol distribution in the Northern Hemisphere during ACE-Asia: Results from global model, satellite observations, and Sunphotometer measurements, J. Geophys. Res., 109, https://doi.org/10.1029/2004JD004829, 2004.

Forrister, H., et al.: Evolution of brown carbon in wildfire plumes, Geophys. Res. Lett., 42, doi:10.1002/2015GL063897, 2015.

Giglio, L., Randerson, J. T., van der Werf, G. R.: Analysis of daily, monthly, and annual burned area using the fourth generation global fire emissions database (GFED4), J. Geophys. Res.-Biogeo, 118, 317–328, https://doi.org/10.1002/jgrg.20042, 2013.

Ginoux, P., Chin, M., Tegen, I., Prospero, J. M., Holben, B., Dubovik, O., Lin, S.-J.: Sources and distribution of dust aerosols simulated with the GOCART model, J. Geophys. Res., 106, doi:10.1029/2000JD000053, 2001.

Guang-Ming,W., Zhi-Yuan, C., Shi-Chang, K., Kawamura, K., Ping-Qing, F., Yu-Lan, F., Xin,W., Shao-Peng, G., Bin, L.: Brown carbon in the cryosphere: Current knowledge and perspective, Environ. Sci. Technol., 7, 82–89, https://doi.org/10.1016/j.accre.2016.06.002, 2016.

Guenther, A., Karl, T., Harley, P., Wiedinmyer, C., Palmer, P. I., and Geron, C.: Estimates of global terrestrial isoprene emissions using MEGAN (Model of Emissions of Gases and Aerosols from Nature), Atmos. Chem. Phys., 6, 3181–3210, https://doi.org/10.5194/acp-6-3181-2006, 2006.

Kok, J. F.: A scaling theory for the size distribution of emitted dust aerosols suggests climate models underestimate the size of the global dust cycle, PNAS, 10, 274–281, https://doi.org/10.1073/pnas.1014798108, 2011.

Kok, J. F., Ridley, D. A., Zhou, Q., Miller, R. L., Zhao, C., Colette, L. H., Ward, D. S., Albani, S., Haustein, K.: Smaller desert dust cooling effect estimated from analysis of dust size and abundance, Nature Geoscience, 10, 274–281, https://doi.org/10.1038/ngeo2912, 2017.

Kuhns, H., Knipping, E. M., and Vukovich, J. M.: Development of a United States–Mexico Emissions Inventory for the Big Bend Regional Aerosol and Visibility Observational (BRAVO) Study, J. Air Waste Manage. Assoc., 55, 677–692, doi:10.1080/10473289.2005.10464648, 2005.

Lambe, A. T., et al.: Relationship between oxidation level and optical properties of secondary organic aerosol, Environ. Sci. Technol., 47, 6349–6357, https://doi.org/10.1021/es401043j, 2013.

Laskin, A., Laskin, J., and Nizkorodov, S. A.: Chemistry of Atmospheric Brown Carbon, Chem. Rev., 115, 4335–4382, https://doi.org/10.1021/cr5006167, 2015.

Lin, G., Penner, J. E., Flanner, M. G., Sillman, S., Xu, L., Zhou, C.: Radiative forcing of organic aerosol in the atmosphere and on snow: Effects of SOA and brown carbon, J. Geophys. Res., 119, 7453–7476, https://doi.org/10.1002/2013JD021186, 2014.

Liu, H. Y., Jacob, D. J.; Bey, I., Yantosca, R. M.: Constraints from Pb-210 and Be-7 on wet deposition and transport in a global three-dimensional chemical tracer model driven by assimilated meteorological fields, J. Geophys. Res., 106, 12109–12128, doi:10.1029/2000jd900839, 2001.

Liu, J., Fan, S., Horowitz, L. W., Levy II, H.: Evaluation of factors controlling long-range transport of black carbon to the Arctic, J. Geophys. Res., 116, https://doi.org/10.1029/2010JD015145, 2011.

Olivier, J. G. J. and Berdowski, J. J. M.: Global emissions sources and sinks, in: The Climate System, edited by: Berdowski, J., Guicherit, R., and Heij, B. J., A. A. Balkema Publishers/Swets & Zeitlinger Publishers, Lisse, the Netherlands, 33–78, 2001.

Park, R. J., Jacob, D. J., Chin, M., Martin, R. V.: Sources of carbonaceous aerosols over the United States and implications for natural visibility, J. Geophys. Res., 108, 4355, https://doi.org/10.1029/2002JD003190, 2003.

Pye, H. O. T., Chan, A. W. H., Barkley, M. P., and Seinfeld, J. H.: Global modeling of organic aerosol: the importance of reactive nitrogen (NO_x and NO_3), Atmos. Chem. Phys., 10, 11261–11276, https://doi.org/10.5194/acp-10-11261-2010, 2010.

Schultz, M., Backman, L., Balkanski, Y., Bjoerndalsaeter, S., Brand, R., Burrows, J., Dalsoeren, S., de Vasconcelos, M., Grodtmann, B., Hauglustaine, D., Heil, A., Hoelzemann, J., Isaksen, I., Kaurola, J., Knorr, W., Ladstaetter-Weissenmayer, A., Mota, B., Oom, D., Pacyna, J., and Wittrock, F.: REanalysis of the TROpospheric chemical composition over the past 40 years, Project ID: EVK2-CT-2002-00170, 2007.

Streets, D. G., Bond, T. C., Carmichael, G. R., Fernandes, S. D., Fu, Q., He, D., Klimont, Z., Nelson, S. M., Tsai, N. Y., Wang, M. Q., Woo, J.-H., and Yarber, K. F.: An inventory of gaseous and primary aerosol emissions in Asia in the year 2000, J. Geophys. Res.-Atmos., 108, 8809, doi:10.1029/2002JD003093, 2003.

Tuccella, P., Curci, G., Pitari, G., Lee, S., Jo, D. S.: Direct radiative effect of absorbing aerosols: sensitivity to mixing state, brown carbon and dust refractive index and shape, J. Geophys. Res., 125, e2019JD030967, https://doi.org/10.1029/2019JD030967, 2020.

Updyke, K. M., Nguyen, T. B., Nizkorodov, S. A.: Formation of brown carbon via reactions of ammonia with secondary organic aerosols from biogenic and anthropogenic precursors, Atmos. Env, 63, 22–31, https://doi.org/10.1016/j.atmosenv.2012.09.012, 2012.

van der Werf, G. R., Randerson, J. T., Giglio, L., Collatz, G. J., Mu, M., Kasibhatla, P. S., Morton, D. C., DeFries, R. S., Jin, Y., and van Leeuwen, T. T.: Global fire emissions and the contribution of deforestation, savanna, forest, agricultural, and peat fires (1997–2009), Atmos. Chem. Phys., 10, 11707–11735, https://doi.org/10.5194/acp-10-11707-2010, 2010.

Vestreng, V., Mareckova, K., Kakareka, S., Malchykhina, A., and Kukharchyk, T.: Inventory Review 2007; Emission Data Reported to LRTAP Convention and NEC Directive, MSC-W Technical Report 1/07, Tech. rep., The Norwegian Meteorological Institute, Oslo, Norway, 2007.

Wang, X., Heald, C. L., Ridley, D. A., Schwarz, J. P., Spackman, J. R., Perring, A. E., Coe, H., Liu, D., and Clarke, A. D.: Exploiting simultaneous observational constraints on mass and absorption to estimate the global direct radiative forcing of black carbon and brown carbon, Atmos. Chem. Phys., 14, 10989–11010, https://doi.org/10.5194/acp-14-10989-2014, 2014.

Wang, X., Heald, C. L., Liu, J., Weber, R. J., Campuzano-Jost, P., Jimenez, J. L., Schwarz, J. P., and Perring, A. E.: Exploring the observational constraints on the simulation of brown carbon, Atmos. Chem. Phys., 18, 635–653, https://doi.org/10.5194/acp-18-635-2018, 2018.

Zender, C. S., Bian, H., Newman, D.: Mineral Dust Entrainment and Deposition (DEAD)model: Description and 1990s dust climatology, J. Geophys. Res., 108, https://doi.org/10.1029/2002JD002775, 2003.

Zhang, L. M., Gong, S. L., Padro, J., Barrie, L.: A sizesegregated particle dry deposition scheme for an atmospheric aerosol module, Atmos. Environ., 35, 2549–560, https://doi.org/10.1016/S1352-2310(00)00326-5, 2001.

Zhang, Y., et al.: Top-of-atmosphere radiative forcing affected by brown carbon in the upper troposphere, Nature Geoscience, 10, 486–489, doi:10.1038/ngeo2960, 2017.

Table S1. Summary of the MACs in NIR band used in the experiments. The units are in m^2/g.

Experiment	**MAC adopted for each radiation-absorbing aerosol species**			
	Fresh FF BC	Aged FF BC	Fresh BF/BB BC	Aged BF/BB BC
CTRL	3.2	4.8	3.5	5.3
BC-H	3.2	6.1	3.5	6.7
BC-L	3.2	3.5	3.5	3.9
	Fresh BF BrC	Aged BF BrC	Fresh BB BrC	Aged BB BrC
CTRL	0.15	0.15	0.15	0.15
BrC-H	0.15	0.15	0.15	0.15
BrC-L	0.15	0.15	0.15	0.15
	Dust 0.36–0.6	Dust 2.6–3.6	Dust 4.4–6.0	Dust 7.0–12.0
CTRL	0.025	0.034	0.029	0.025
DUST-H	0.031	0.040	0.034	0.029
DUST-L	0.014	0.020	0.018	0.016

Table S2. Comparison of measured and modelled BC and BCE median mixing ratio in surface snow. The units are in ng/g.

Region	Period	BC Observed	BC Modelled	BCE Observed	BCE Modelled
Arctic[1]					
Arctic Ocean, spring	2005-2008	7±3	9	12±5	16
Arctic Ocean, summer	2005-2008	8±8	7	14±15	11
Canadian and Alaskan Arctic	Apr.-May 2007-2009	8±3	7	14±7	11
Canadian sub-Arctic	Mar.-Apr. 2009	14±9	8	20±12	12
Greenland, spring	Apr. 2009	4±2	6	7±3	8
Greenland, summer	2006-2008	1±1	7	3±3	11
Western Russia	Mar.-May 2007	27* (12-48)**	18	34* (15-60)**	32
Eastern Russia	Mar.-May 2008	34±46	11	48±90	20
Svalbard	Mar.-Apr. 2007, 2009	13±9	11	18±12	15
Tromso, Norway	May 2008	21±12	17	29±16	25
Antarctica					
Vostok[2]	Dec. 1990-Feb. 1991	0.60*	0.61	-	-
Simple Dome[3]	1982-1985	2.5 (2.3-2.9)**	0.38	-	-
South Pole[4]	Jan.-Feb. 1996	0.23* (0.10-0.34)**	0.37	-	-
Sea Ice[5]	Sep.-Nov. 2012	0.30±0.20	0.53	0.40±0.30	0.80
North America[6]					
Pacific Northwest	Jan.-Mar. 2013	22±44	13	29±52	15
Intramountain Northwest	Jan.-Mar. 2013	24±34	28	37±93	35
North U.S. Plains	Jan.-Mar. 2013	30±54	37	78±245	39
Canada	Jan.-Mar. 2013	15±13	15	25±45	18
Northwest China[7]					
Northern Xinjiang	Jan.-Feb. 2012	73 ± 120	61	-	-
Northeast China[8]					
Qilian Mountains	Jan.-Feb. 2010	-	-	1550* (426-3042)**	493
Inner Mongolia	Jan.-Feb. 2010	340±910	338	820±3060	1057
Northeast border	Jan.-Feb. 2010	135* (68-295)**	68	190* (100-374)**	98
Industrial Northeast	Jan.-Feb. 2010	1220±600	436	1720±840	556
Himalayas and Tibet Plateau[9]					
Hilamalayas, summer	2000-2001	21* (0.3-43)**	48	-	-
Tibet Plateau, summer	2001	45* (18-446)**	26	-	-

[1] Doherty et al. (2010)

[2] Grenfell et al. (1994)

[3] Chylek et al. (1987)

[4] Warren and Clark (1990)

[5] Zatko and Warren (2015)

[6] Doherty et al. (2014)

[7] Ye et al. (2012)

[8] Wang et al. (2013)

[9] Kopacz et al. (2011)

[*] Average

[**] The standard deviations are not available. The values in the brackets represent the low-high range measured in the region.

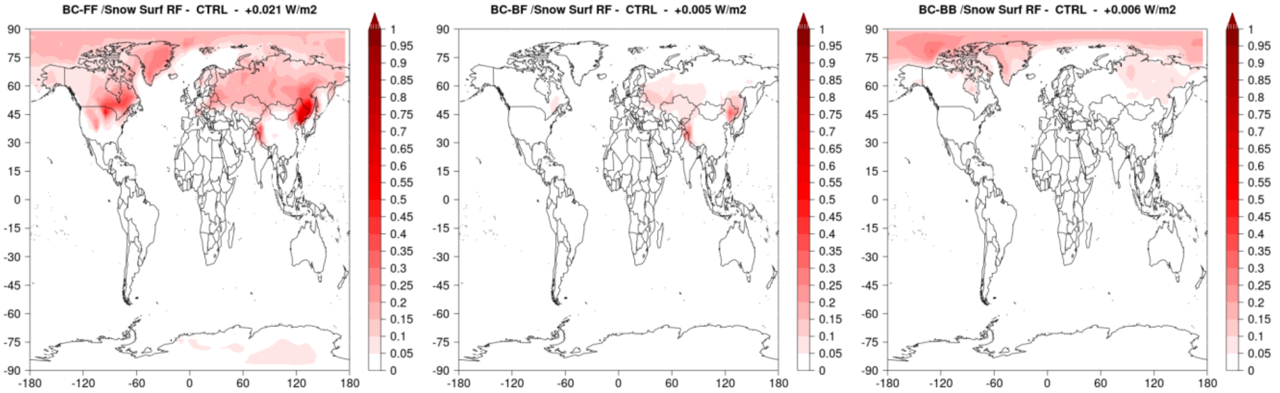

BC-FF /Snow Surf RF - CTRL - +0.021 W/m2

BC-BF /Snow Surf RF - CTRL - +0.005 W/m2

BC-BB /Snow Surf RF - CTRL - +0.006 W/m2

Figure S1. All-sky annual mean (2010–2014) black carbon snow RF divided by source (FF=fossil fuel, BF=biofuel, BB=biomass burning).

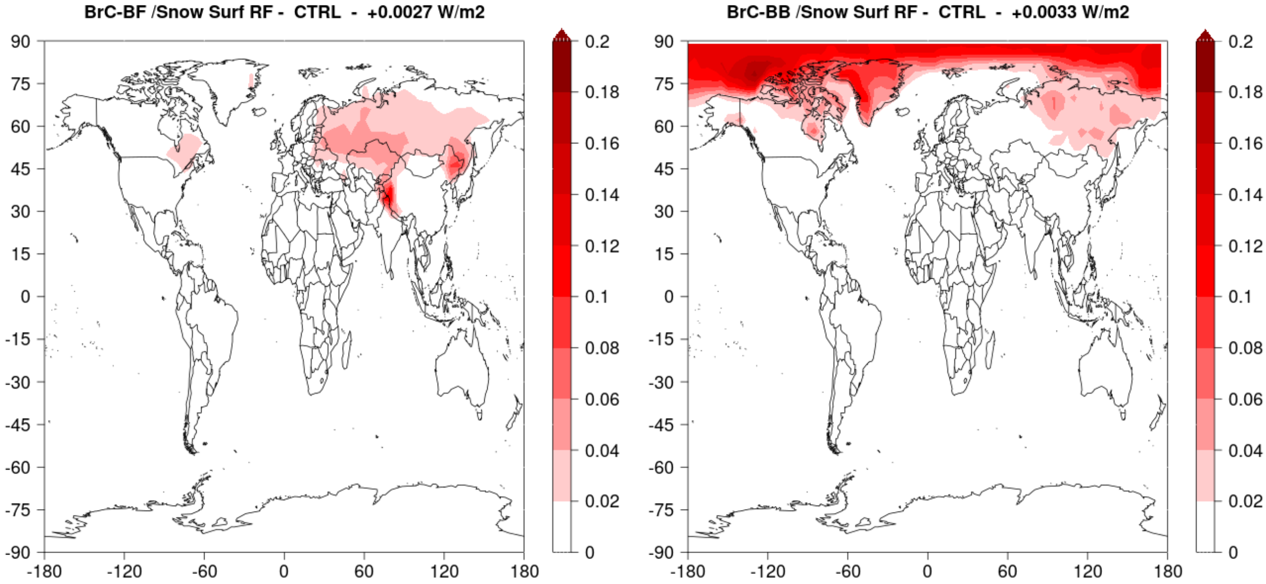

BrC-BF /Snow Surf RF - CTRL - +0.0027 W/m2

BrC-BB /Snow Surf RF - CTRL - +0.0033 W/m2

Figure S2. **Same as Figure S1, but for brown carbon.**

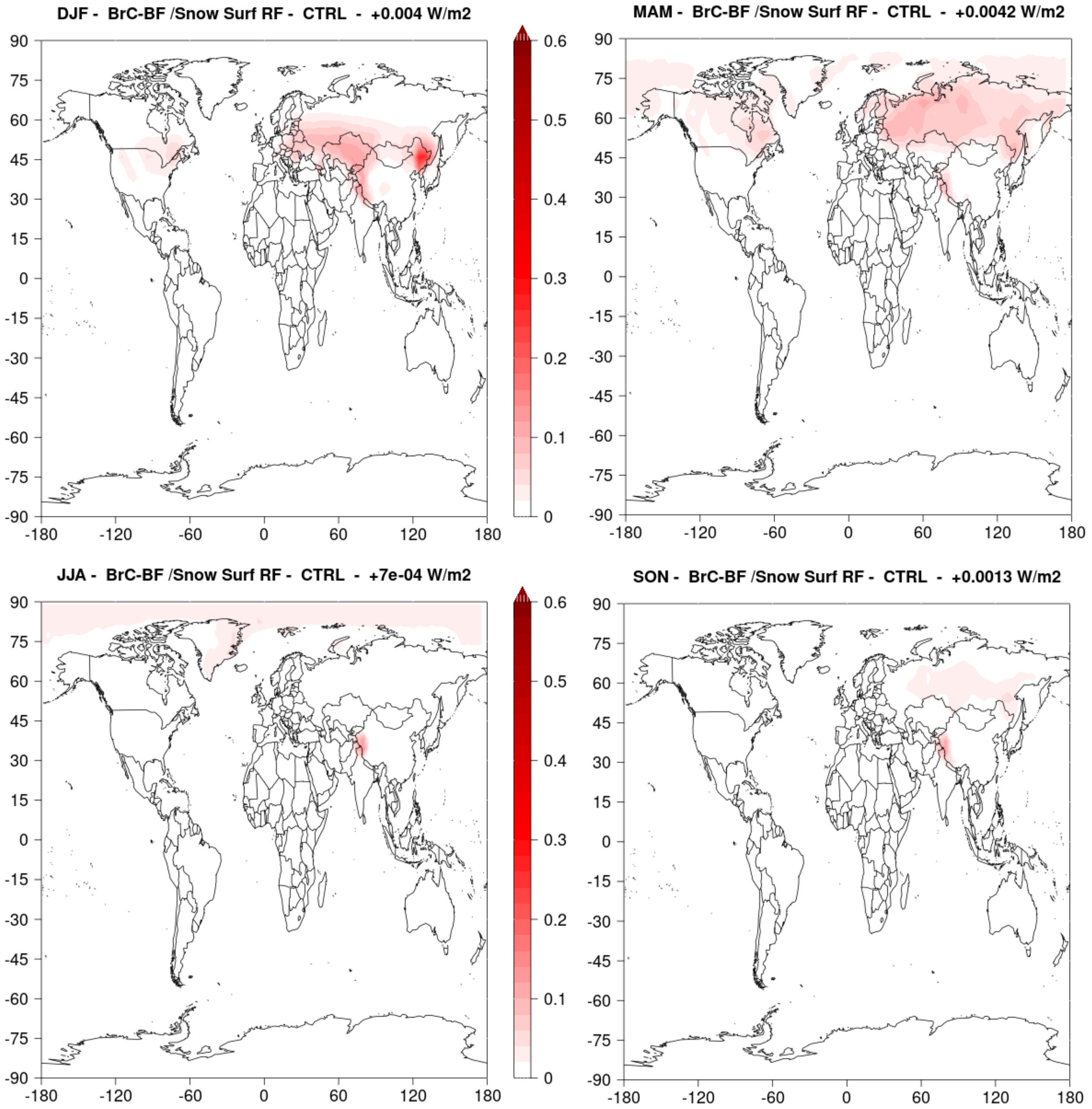

Figure S3. All-sky annual mean (2010–2014) of seasonal BrC-BF snow RF.

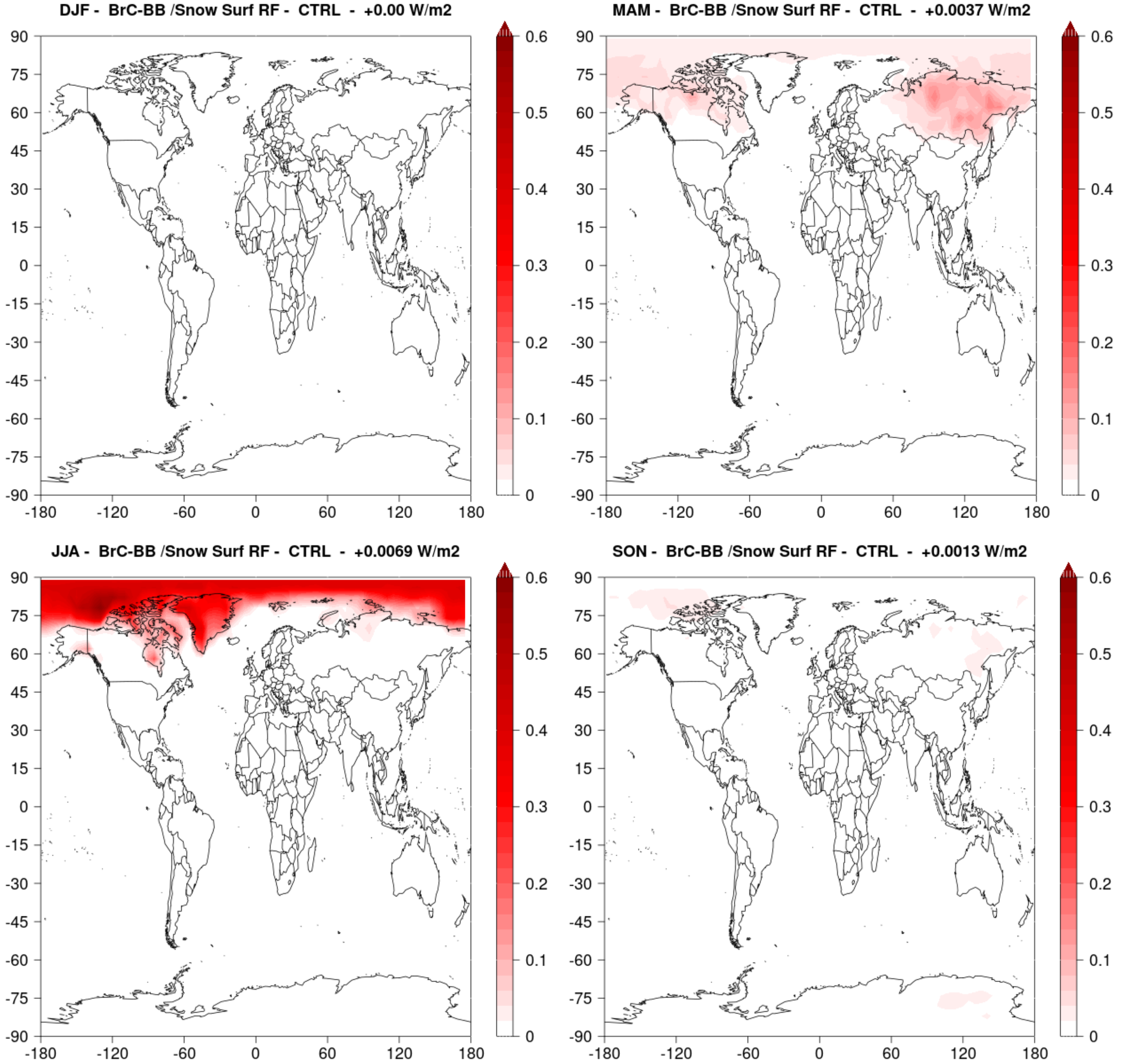

Figure S4. All-sky annual mean (2010–2014) of seasonal BrC-BB snow RF.

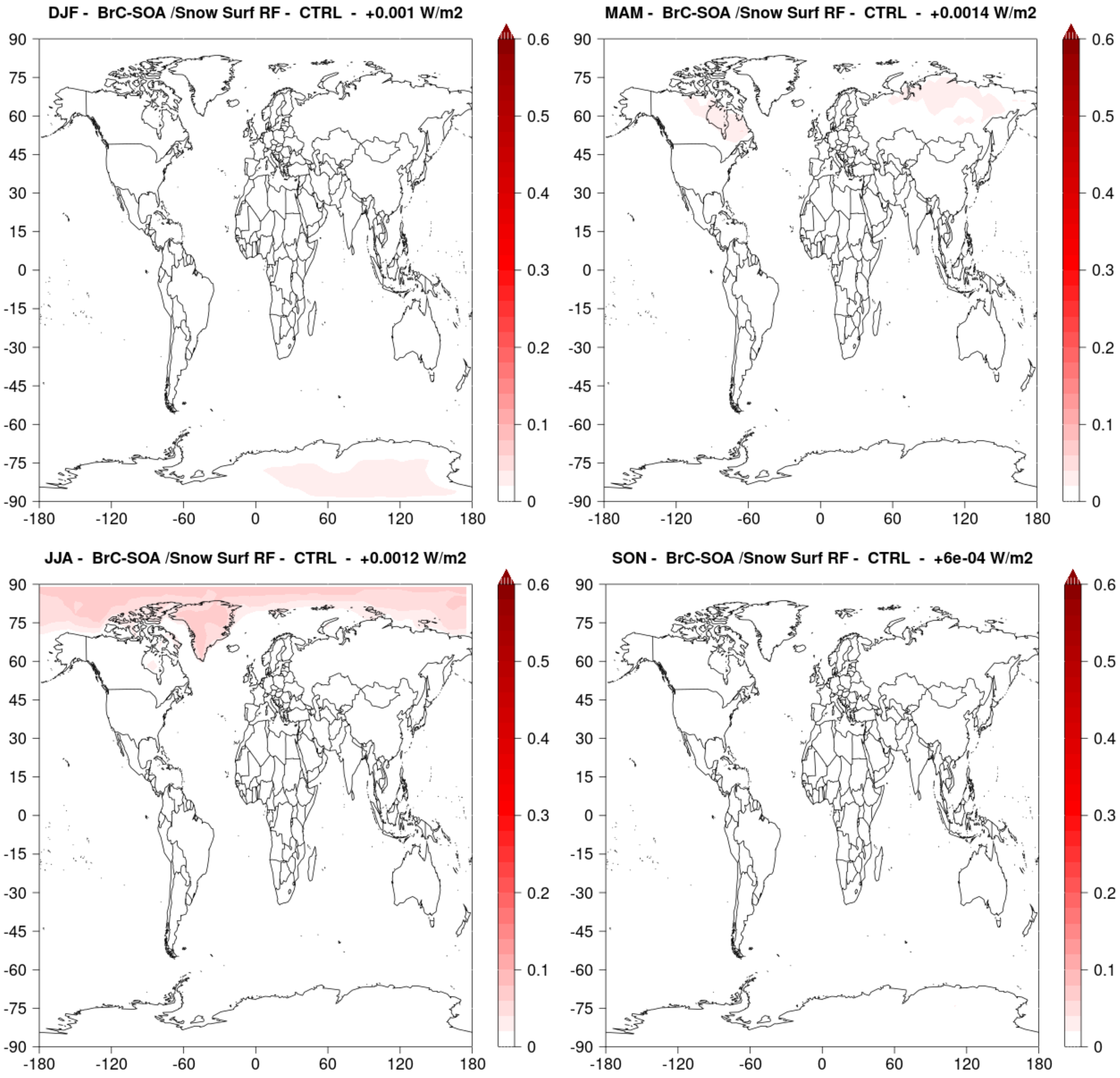

Figure S5. All-sky annual mean (2010–2014) of seasonal BrC-SOA snow RF.

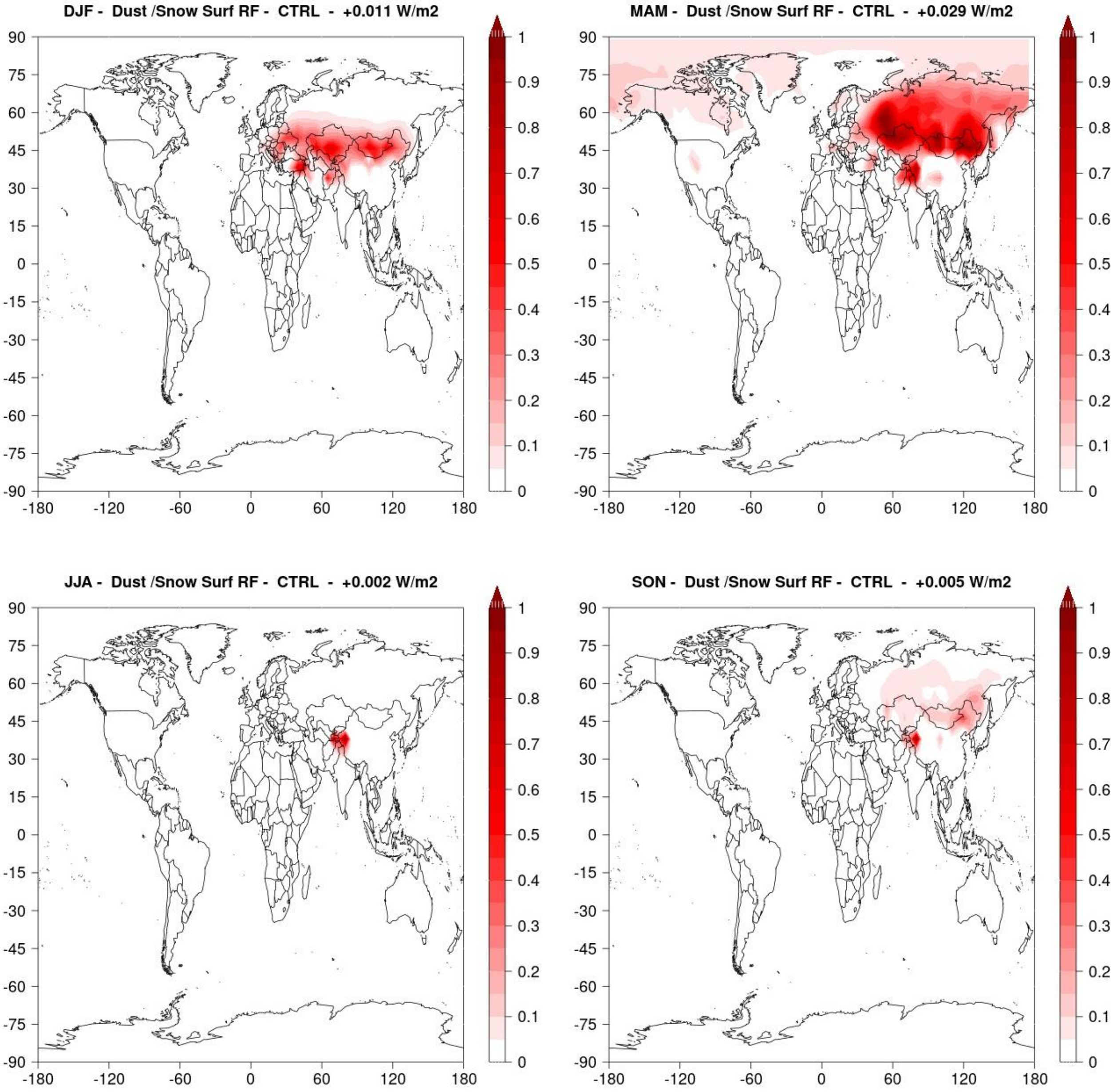

Figure S6. All-sky annual mean (2010–2014) of seasonal soil dust snow RF.